13th Australia New Zealand Conference on Geomechanics – Acosta-Martínez & Lehane (Eds.)

Mechanical characterisation of a highly friable weak sandstone

M. Khoshini, A. Khoshghalb, H. Moghaddasi & N. Khalili
School of Civil and Environmental Engineering, UNSW Sydney, Sydney, Australia

ABSTRACT: Leura weak sandstone is one of the most dominating surface rocks in the Sydney Basin. Many infrastructure construction practices are to be dealt with this heavily eroded quartzose porous sandstone (void ratio of 0.3) with complex yet overlooked behaviour as it lies in the transition zone between soils and rocks. The material is problematic from the first steps of characterisation as obtaining good-quality undisturbed samples from the rock mass is difficult which gets even more complicated considering the high heterogeneity of the rock mass. This study concerns full characterisation of the Leura weak sandstone. A method for dry core drilling of the material and sample preparation is introduced to obtain high-quality undisturbed core samples. These samples are then used to evaluate the engineering properties (gradation, void ratio, density, unconfined compression strength, and permeability) and mechanical behaviour of the material. Triaxial compression and isotropic compression tests under a wide range of confining pressures (0 to 100 MPa) are conducted to investigate the mechanical response of the material. The results show that failure mode is brittle for confining pressures less than 3MPa, while for higher confining pressures, cataclastic failure mode is observed. The yield locus and the plastic potential of the material is captured for a range of confining pressures. The effect of structure on the compressive behaviour of the material under isotropic loading, which is of prominent importance for bonded geomaterials, is captured by means of isotropic compression tests. Consolidated drained triaxial tests are also conducted on the material in the fully de-structured state to capture the yield locus, flow rule, and the critical state parameters of the base materials. Understanding the mechanical properties of the fully de-structured state of the material is crucial to incorporate advanced constitutive models to capture the behaviour of the structured material.

1 INTRODUCTION

The University of New South Wales (UNSW) was engaged to conduct research on the development of procedures for cost-effective design of cut batters, soil nailing, retaining structures and bridge foundations in low strength rocks encountered in the Upper Blue Mountain region of NSW. As part of this research work, extensive experimental investigations have been carried out on Leura weak sandstone, hereby abbreviated as LWSS, for the purpose of rock characterisation and parameter identification of constitutive modelling.

In this paper, the laboratory investigation to obtain the engineering and mechanical properties of the material is presented. This includes detailed account of in-situ sampling and sample preparation, grain size distribution, mass and volumetric properties of the material, permeability, slake durability, unconfined compressive strength (UCS), as well as triaxial compression tests and isotropic compression tests at a suite of confining pressures.

2 NATURAL WEAK SANDSTONE

The material is a weak sandstone of Leura region, NSW, Australia. The rock mass is white to amber coloured with visible bedding layers and a grainy rough surface that is highly weathered at shallow depths, very friable, and susceptible to mechanical and moisture degradation (Figure 1).
LWSS comprises sub-rounded to sub-angular quartz grains embedded in a clay matrix reacted with lime with occasional yellow iron oxidation. This rock outcrops in the Katoomba region (abbreviated as *Rnw* in the geological map of the Katoomba region

Figure 1. Cut face of the LWSS

and *Rn* in the geological map of the Sydney basin) generally underlays the Hawkesbury sandstone in the Sydney basin.

Based on the X-ray diffraction (XRD) analysis, minerals forming the weak sandstone consists of 84-91% of quartz (SiO_2), 7-12% of Kaolinite ($Al_2\ Si_2\ O_5\ (OH)_4$) and 2-4% of Aragonite ($CaCO_3$). Observations made through scanning electron microscopy (SEM) to examine the microstructure of the material show that the coarse angular quartz grains are embedded in cement agent consisting mainly of lime-reacted as well as fresh clay minerals. The pore space is mainly interconnected ranging from a millimetre to microns in size (Figure 2).

3 SAMPLE PREPARATION

3.1 *Coring*

None of the conventional methods of core drilling could be applied for sampling the rock mass as the material is extremely friable. Sample blocks of the sandstone were dug and cut from the site then transferred to the laboratory. Wet core drilling and cutting were found to be impractical as the fabric of the stone is completely disintegrated as it was exposed to the water used as coolant liquid. Moreover, the material was very weak and susceptible to degradation under the cutting action of the coring bit. After numerous unsuccessful attempts, examining different methods of coring, water freeze coring was found as the only practical option to obtain representative samples of the sandstone. Frozen water provided a secondary support between the rock grains through the interconnected pore space of the material fortifying the weak sandstone to retain its integrity during the coring process. The degree of saturation of the rock at 3% water content was between 25% to 35%. Therefore, due to the low moisture content of the blocks, the freezing process does not affect the pore structure of the rock and the bonds between the sand grains. Cylindrical specimens were cored out of the frozen blocks using a costume-made dry core drill bit mounted on a specialized coring machine. The drilling machine was equipped with a gearbox allowing operator-controlled speed on a continuous range from 0-150 rpm. To achieve minimal disturbance, the coring was commenced from a very low rotating speed of about 60 rpm and after 2 cm of penetration, the rotation speed was increased gradually to 150 rpm. A strong vacuum was used to extract the accumulated dust from the drill bit to avoid clogging. No coolant/lubricating liquids were used due to the friable nature of the rock.

3.2 *End preparation and effects*

Good quality cores of the material were trimmed to the desired length to diameter ratio (L/D) of 2.0-2.5 according to ASTM D7012 (2010). The ends of the cores were flattened to the extent possible using a pallet knife and coarse brush. ISRM (1972) guidelines discourage the use of capping materials or any end surface treatments other than machining. This is due to uncertainties associated with the capping materials induced shear and friction at the loading interfaces, and the resulting impact on the failure stress (Ulusay, 2015). For hard rocks, i.e. rocks with a UCS greater than 50 MPa, it is difficult to find a capping material capable of matching the mechanical properties of the test rock. However, as pointed out by Hudson (2014), for friable rocks, end capping would be the only option to obtain a test specimen that can produce reliable results. He suggested a capping material with a similar stiffness and greater strength than the test material to be used for weak rocks.

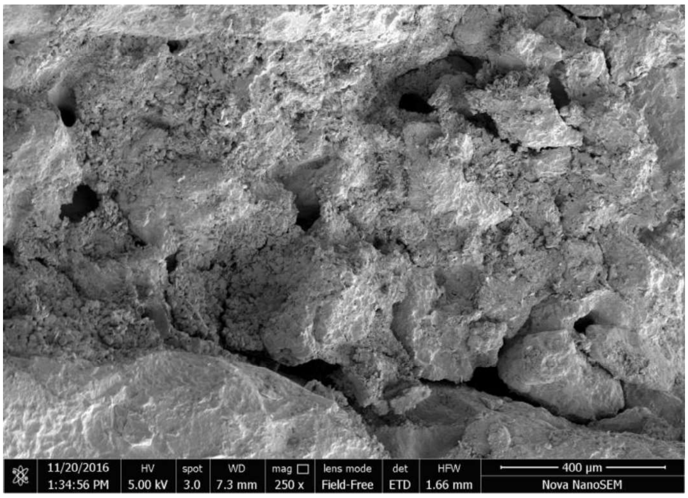

Figure 2. SEM image of the LWSS showing grains, bonds, pores, and cracks

A mixture of a fast-setting cement paste (Conbextra HES with the water to cement ratio of 0.3 by weight) and a fine sand, consisting of crushed natural sandstone grains passing through a 600µm sieve and retained on a 300µm sieve, was used. This forms a workable porous paste suitable for capping with good adhesion to the sandstone, high stiffness and high permeability. Using the capping paste, the specimen ends were prepared flat to ±0.02mm and made perpendicular to its axis to the accuracy of ±0.05mm in 50 mm as suggested by ISRM.

To evaluate the strength, stiffness and the effect of the capping material on the mechanical response of the sandstone, cylindrical samples of the capping paste, 50mm in diameter and 100mm in height, were prepared. Samples were cured for 24 hours and then subjected to the UCS testing. A total of 3 specimens were tested yielding the average tangent uniaxial elasticity modulus and UCS values of 423 MPa and 16 MPa, respectively. While the strength of the capping material was considered as acceptable, its uniaxial modulus of elasticity was not high enough to exclude its effect on the axial strains recorded. To eliminate the effect of the low stiffness of the capping material, a correction procedure was established to calculate the axial strain of the sandstone, ε_{as}, from the measured axial strain using equation (1) as follows

$$\varepsilon_{as} = \frac{q(\frac{L_t}{E_t} - \frac{l_c}{E_c})}{L_s} \quad or \quad E_s = \frac{L_s}{(\frac{L_t}{E_t} - \frac{l_c}{E_c})} \tag{1}$$

where l_c, L_s and L_t are the thickness of the capping material, the length of sandstone material and the total length of the capped specimen, respectively. q stands for the applied deviatoric stress, E_t is the total uniaxial elasticity modulus measured during the test, E_c is the uniaxial elasticity modulus of the capping material, and E_s is the corrected uniaxial elasticity modulus of the sandstone. Results of the tests conducted on capped specimens were corrected for the stiffness of the capping material using Equation (1). Adopting such capping practice alongside the strain/stiffness correction method is highly recommended for sample preparation of weathered or very weak rock samples.

4 ENGINEERING PROPERTIES

4.1 *Gradation, density, and porosity*

The grain size distribution of the de-structured (remoulded) state of the sandstone can be described as well graded sand with 10-15% fines. The coefficient of uniformity, Cu, is 7.1 and the coefficient of curvature, Cc, is 1.53.

Specific gravity, G_s, of the grains was 2.63 measured according to ASTM D854. Dry density, γ_d, of several lumps of the intact material was measured using the ISRM water displacement method (Ulusay, 2015). Oven dried lumps of the sandstone were weighed and then coated with a very thin layer of epoxy to make them impermeable. Bulk volume of the lumps was then measured from the volume of water displaced with coated lumps. Knowing the weight of the coating epoxy, the bulk volume was corrected. The difference between the corrected and uncorrected bulk volume was less than 0.05%. Average dry density and void ratio of the LWSS were obtained as $\gamma_d = 19.92$ kN/m^3 and $e = 0.32$ (porosity=0.24).

4.2 *Unconfined compressive strength*

A total of eight UCS tests were performed on the LWSS using a loading frame equipped with a 500kN loadcell. In accordance with ISRM (1974-2006) (Hatheway, 2009), two LVDTs (Linear Variable Differential Transducer) were used for logging the axial deformation. A circumferential chain setup with a 12mm-range displacement measurement transducer was used to capture the radial deformations. The UCS values obtained, σ_c, ranged from 1.01 to 4.17 MPa with an average value of 2.75 MPa and a standard deviation of 0.94 MPa. Tangent elasticity modulus measured at $0.5\sigma_c$ ranged from 227.98 to 793.25 MPa with an average value of 477.94 MPa. Stress-strain curves and axial stress versus radial strain of the samples are shown in Figure 3.

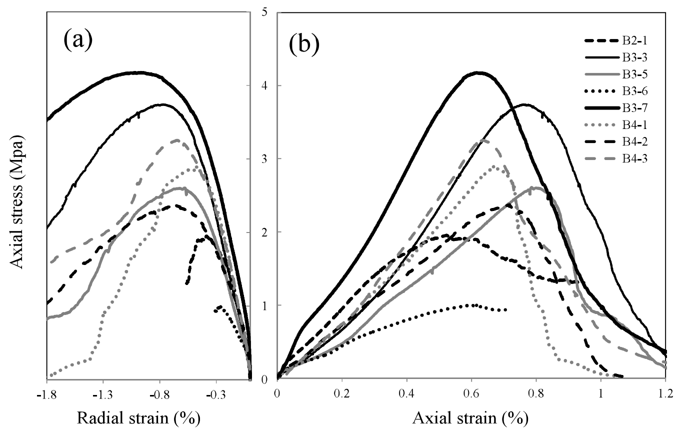

Figure 3. The response of the LWSS under uniaxial compression test: Axial stress versus (a) radial strain and (b) axial strain for eight samples of the LWSS.

5 MECHANICAL PROPERTIES

5.1 *Triaxial compression tests – Remoulded state*

A general feature of the response in porous media is that loose materials contract whereas dense materials expand during shearing towards failure. In other words, in sands and clays, contraction is observed in their loose and normally consolidated states, whereas expansion is observed for dense sands and overconsolidated clays. In each case, the deformation tends towards a state where no further volume change occurs upon shearing; this state is denoted as the *critical state* (Schofield and Wroth, 1968). At critical state, the shearing resistance is independent of the past stress history and is only a function of the current stresses applied to the material (Russell and Khalili, 2002). The critical state is also associated with the fully de-structured and remoulded state of the material.

In order to obtain critical state parameters of the LWSS, a block of the material was crushed into its constituent particles with a rubber pestle and mortar. Cylindrical specimens of the crushed rock, 50mm in diameter and 100mm in height and initial target void ratio of 0.4 were prepared. Upon saturation, the samples were tested under the consolidated-drained triaxial condition under different confining pressures. Figure 4 shows the behaviour of the de-structured LWSS on the deviatoric stress-axial strain, $q-\varepsilon_a$, and volumetric strain-axial strain, $\varepsilon_v - \varepsilon_a$, planes. Compression is shown negative in this figure. Tests were continued to large axial strains in order to capture the critical state parameters. Deviatoric stress, q, and its corresponding effective volumetric stress, p', at peak and critical state were obtained from $q-\varepsilon_a$ and $\varepsilon_v - \varepsilon_a$ diagrams which were then used to plot the peak and critical state lines in the $q-p'$ plane. The critical state line is represented by $q = Mp' + a$ on the $q-p'$ plane (Figure 5) (Atkinson and Bransby, 1977). The critical state parameter obtained is $M = 1.34$ and $a = 0$, corresponding to the critical state effective cohesion, c'_{cr}, of zero and critical state friction angle, φ'_{cr}, of 33.2 degrees. For the peak state, M and a are 1.45 and 39 kPa, respectively; corresponding to the peak effective cohesion, c'_{peak}, of 19.5 kPa, and peak friction angle, φ'_{peak}, of 35.78 degrees.

5.2 *Triaxial compression test-intact samples*

In order to obtain mechanical parameters of the material under shear, consolidated drained triaxial compression tests were performed on intact specimens of the weak sandstone. Particular attention was given to accurate measurement of volume change of the sample during deviatoric loading. Volume change measurements are crucial for the determination of flow rule, hardening rule, plastic potential and critical state parameters of the rock when the volume change of the sample tends to zero.

Low-confining-pressure triaxial tests were conducted using a GDS stress path triaxial apparatus. The apparatus comprises a loading frame, pressure cell, cell pressure controller and back pressure controller. It has a rated maximum confining pressure of 3.5MPa, maximum back pressure of 1MPa, and maximum axial loading of 50kN. The load cell is accurate to ±0.1% of the full range output (50N). The back pressure controller is capable of measuring the volume change during each test with a precision of ±1 mm^3. Axial displacement of the system was measured using a linear potentiometer displacement transducer (LPDT) with a maximum range of 50mm and precision of $\pm 10^{-4}$ mm. In addition to these measurements, two axial and one radial on-sample transducers were used to measure the deformation of the sample during each test. Tests under higher confining pressures were conducted by a rock triaxial cell placed in the frame used for the UCS tests. The rock triaxial cell is capable of applying the confining pressures up to 70 MPa and is equipped with local LVDTs to measure the radial deformations of the test sample.

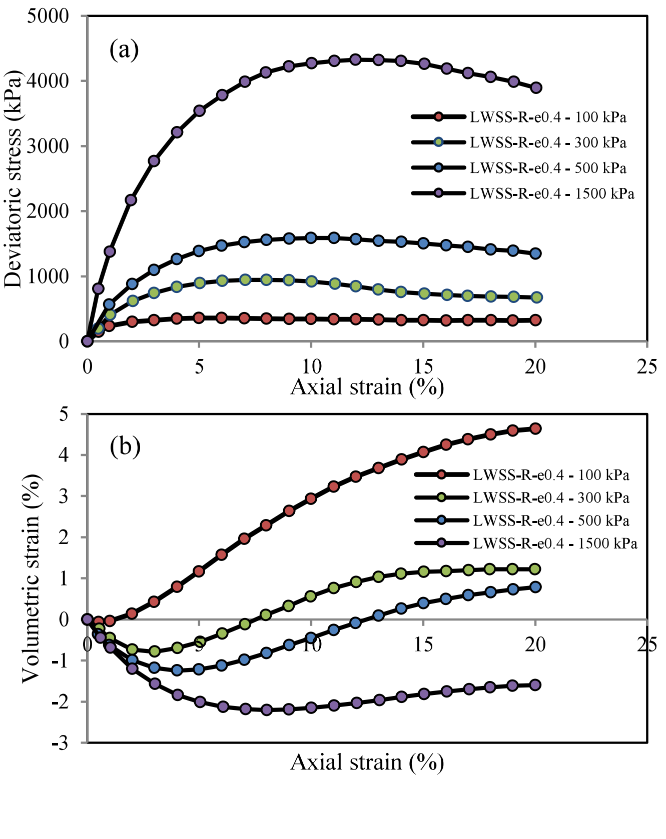

Figure 4. Consolidated-drained triaxial test on the remoulded samples of the LWSS: (a) stress-strain curves and (b) volumetric change behaviour

Specimens of the material were tested under confining pressures of 300, 800, and 1500 kPa by the GDS stress path triaxial cell and 5, 10, and 15 MPa by the rock triaxial cell along axial compression stress path. The consolidated-drained triaxial compression tests were conducted on samples obtained from different blocks with initial void ratios ranging from 0.23 to 0.35. Deviatoric stresses obtained at the peak and critical state for confining pressure of 300 kPa ranged from 3264 to 6435 kPa for the peak strength and 2502 to 3829 kPa for the critical state strength. For the confining pressure of 1500 kPa, deviatoric stresses ranged from 10105 to 16109 kPa for peak strength and 7869 to 11645 kPa for the critical state. In these low confining stresses, the prevailing mode of failure is brittle with considerable post-peak softening. All samples tested, exhibited dilatant behaviour, and localized deformation with shear movements along specific shear bands. The stress-strain curves and the volume change under shear for representative triaxial tests under confining pressures of up to 1500 kPa are plotted in Figure 6. Void ratios are 0.24, 0.23, and 0.25 for the test samples under confinings of 1500, 800, and 300 kPa respectively.

The same procedure as that of the remoulded samples was used to derive the peak parameters of the intact samples. Deviatoric and mean effective stresses at peak under triaxial compression are also plotted in Figure 5. For the peak state, M is 2.13, corresponding to a peak effective friction angle of φ'_{peak}= 52 degrees. In the case of intact samples, a q-intersection of $a = 70\ kPa$ is also observed in the $q-p'$ plane, corresponding to a peak effective cohesion of c'_{peak}= 40 kPa. Note that obtaining critical state parameters from testing intact rocks could be questionable due to the strain localization phenomena. In fact, only a restricted zone of the material along the shear plane undergoes a quasi-critical state condition and the other regions of the sample remain intact.

5.3 *Isotropic compression tests*

The rock triaxial cell is also used to compress samples of intact rock isotropically from nil to elevated pressures where either the pressure reaches the cell capacity or the cell oil leaks into the sample. On such a stress path, the material collapse due to pure isotropic pressure can be captured as an abrupt increase in the compression rate of the material. This is the onset of structure collapse or bond degradation in structured geomaterials (Maccarini (1987), Leroueil and Vaughan (1990), and Lagioia and Nova (1995)). Such collapse can be seen in Figure 7 where the specific volume of the test samples is plotted against the mean effective stress in a semi-logarithmic plane.

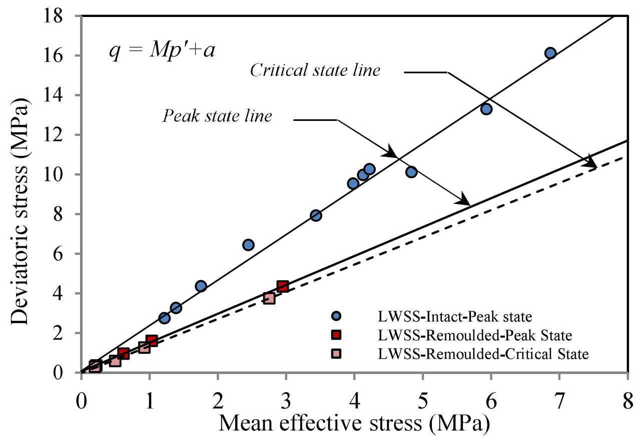

Figure 5. Extracting the peak and critical state parameters

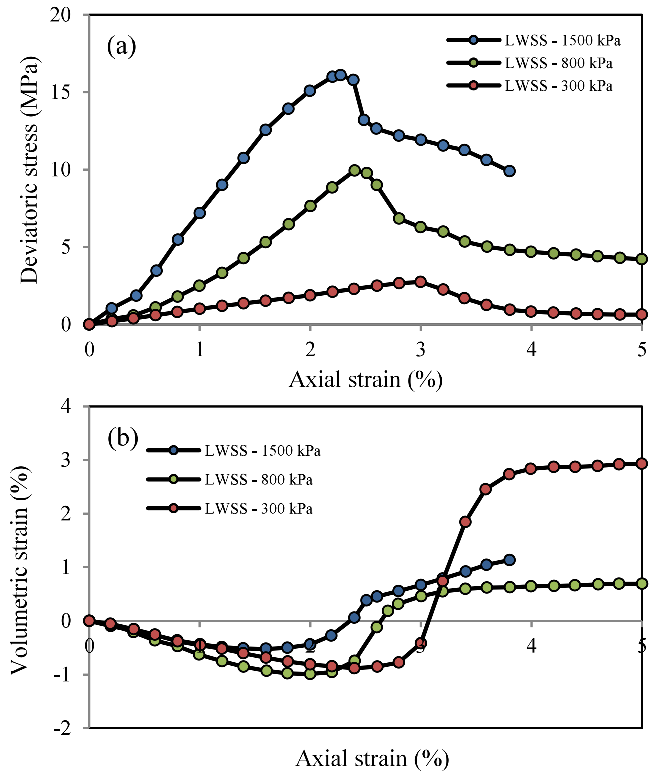

Figure 6. Consolidated-drained triaxial test on intact samples of the LWSS: (a) stress-strain curves and (b) volumetric change behaviour

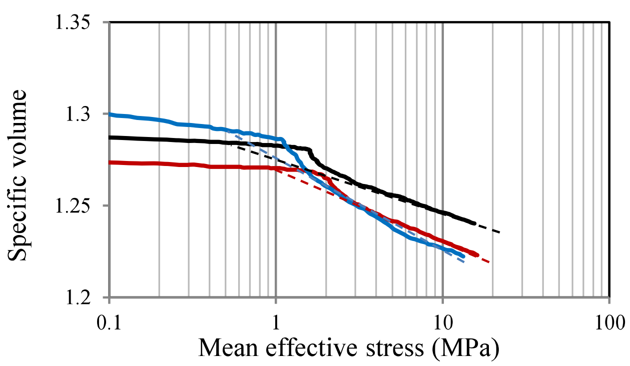

Figure 7. Isotropic compression test results on three samples of the LWSS.

6 YIELD SURFACE

Yield state for geomaterials is generally defined as the point of an abrupt change in the stiffness on their stress path. This is captured by different researchers in different ways (Sangrey (1972), Ishihara and Okada (1978), Maccarini (1987), Leroueil and Vaughan (1990), and Cotecchia and Chandler (2000)). In this study, the peak stress in the brittle failure stage is taken as the yield point for the samples under low confining pressure. For the ductile failure mode, the end of the initial semi-linear stress-strain behaviour gives reasonable stresses for the yield point. Under the isotropic compression, the pressure at which bond degradation happens is assumed as the yielding point. The yield points of the remoulded and intact samples of the LWSS are plotted on the $q - p'$ plane in Figure 8. Also included in this figure are estimations of the yield surface for both intact and remoulded states of the LWSS based on the experimental data, and the equation proposed in (Khalili et al., 2005).

7 CONCLUSION

The paper reports on the experimental investigations conducted to characterize the Leura weak sandstone. The material was tested for engineering and mechanical properties. The following aspects were studied:

- Geology, chemical decomposition and micro-structure
- Gradation, density, and porosity
- Unconfined compressive strength and stiffness
- Triaxial stress-strain and volumetric change response of the intact and remoulded state of the material under a wide range of confining pressures
- Deformation under isotropic compression loading and the onset of structure collapse
- Yield locus of the material

Such information paves the way for development and calibration of constitutive laws needed for numerical modelling of the LWSS in practical applications in particular, and any attempt to numerically predict the behaviour of structured geomaterials in general.

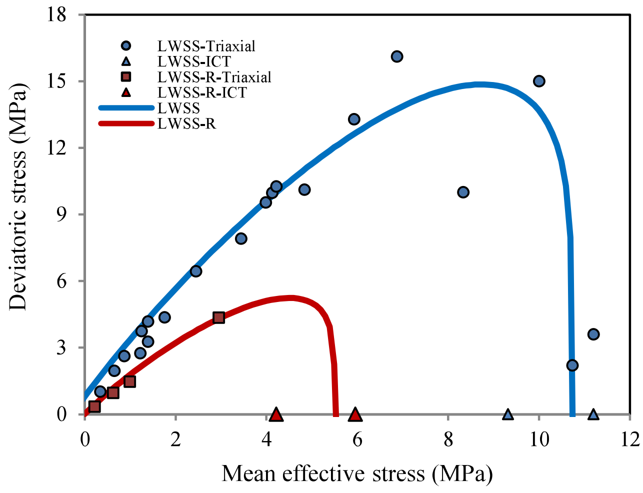

Figure 8. Yield surface for intact and remoulded state of the LWSS using the UNSW bounding surface model

REFERENCES

ATKINSON, J. H. & BRANSBY, P. 1977. The mechanics of soils, an introduction to critical state soil mechanics.

COTECCHIA, F. & CHANDLER, R. 2000. A general framework for the mechanical behaviour of clays. *Géotechnique,* 50**,** 431-448.

HATHEWAY, A. W. 2009. The complete ISRM suggested methods for rock characterization, testing and monitoring; 1974–2006. Assoc Eng Geologists.

HUDSON, J. A. 2014. *Rock Testing and Site Characterization: Comprehensive Rock Engineering:: Principles, Practice and Projects*, Elsevier.

ISHIHARA, K. & OKADA, S. 1978. Yielding of overconsolidated sand and liquefaction model under cyclic stresses. *Soils and Foundations,* 18**,** 57-72.

KHALILI, N., HABTE, M. & VALLIAPPAN, S. 2005. A bounding surface plasticity model for cyclic loading of granular soils. *International journal for numerical methods in engineering,* 63**,** 1939-1960.

LAGIOIA, R. & NOVA, R. 1995. An experimental and theoretical study of the behaviour of a calcarenite in triaxial compression. *Géotechnique,* 45**,** 633-648.

LEROUEIL, S. & VAUGHAN, P. R. 1990. The general and congruent effects of structure in natural soils and weak rocks. *Géotechnique,* 40**,** 467-488.

MACCARINI, M. 1987. Laboratory studies for a weakly bonded artificial soil.

RUSSELL, A. & KHALILI, N. 2002. Drained cavity expansion in sands exhibiting particle crushing. *International Journal for Numerical and Analytical Methods in Geomechanics,* 26**,** 323-340.

SANGREY, D. 1972. Naturally cemented sensitive soils. *Geotechnique,* 22**,** 139-152.

SCHOFIELD, A. & WROTH, P. 1968. Critical state soil mechanics.

ULUSAY, R. 2015. *The ISRM Suggested Methods for Rock Characterization, Testing and Monitoring: 2007-2014*, Springer.